Systems/Circuits

The 5-HT$_{5A}$ Receptor Regulates Excitability in the Auditory Startle Circuit: Functional Implications for Sensorimotor Gating

Paul C. P. Curtin,[1] Violeta Medan,[2] Heike Neumeister,[2] Daniel R. Bronson,[1] and Thomas Preuss[3]

[1]Graduate Center, [2]Research Foundation, and [3]Hunter College, City University of New York, New York, New York 10065

Here we applied behavioral testing, pharmacology, and *in vivo* electrophysiology to determine the function of the serotonin 5-HT$_{5A}$ receptor in goldfish startle plasticity and sensorimotor gating. In an initial series of behavioral experiments, we characterized the effects of a selective 5-HT$_{5A}$ antagonist, SB-699551 (3-cyclopentyl-*N*-[2-(dimethylamino)ethyl]-*N*-[(4′-{[(2-phenylethyl)amino]methyl}-4-biphenylyl)methyl]propanamide dihydrochloride), on prepulse inhibition of the acoustic startle response. Those experiments showed a dose-dependent decline in startle rates in prepulse conditions. Subsequent behavioral experiments showed that SB-699551 also reduced baseline startle rates (i.e., without prepulse). To determine the cellular mechanisms underlying these behaviors, we tested the effects of two distinct selective 5-HT$_{5A}$ antagonists, SB-699551 and A-843277 (*N*-(2,6-dimethoxybenzyl)-*N*′[4-(4-fluorophenyl)thiazol-2-yl]guanidine), on the intrinsic membrane properties and synaptic sound response of the Mauthner cell (M-cell), the decision-making neuron of the startle circuit. Auditory-evoked postsynaptic potentials recorded in the M-cell were similarly attenuated after treatment with either 5-HT$_{5A}$ antagonist (SB-699551, 26.41 ± 3.98% reduction; A-843277, 17.52 ± 6.24% reduction). This attenuation was produced by a tonic (intrinsic) reduction in M-cell input resistance, likely mediated by a Cl$^-$ conductance, that added to the extrinsic inhibition produced by an auditory prepulse. Interestingly, the effector mechanisms underlying neural prepulse inhibition itself were unaffected by antagonist treatment. In summary, these results provide an *in vivo* electrophysiological characterization of the 5-HT$_{5A}$ receptor and its behavioral relevance and provide a new perspective on the interaction of intrinsic and extrinsic modulatory mechanisms in startle plasticity and sensorimotor gating.

Introduction

Serotonin (5-HT) contributes to sensorimotor integration and decision-making by directly and indirectly regulating excitability. The functional plasticity of 5-HT is facilitated by 14 discrete receptor subtypes comprising seven homologous receptor families (5-HT$_1$–5-HT$_7$) (Barnes and Sharp, 1999; Filip and Bader, 2009). Among these, the 5-HT$_{5A}$ receptor has proven remarkably challenging to characterize because of the limited availability of selective ligands (Nelson, 2004; Thomas, 2006; Kassai et al., 2012). The

5-HT$_{5A}$ receptor is nonetheless broadly distributed in the CNS and was recently functionally characterized in native rodent tissues *ex vivo* (Goodfellow et al., 2012), emphasizing the importance of resolving its functionality *in vivo*. Here we studied the function of the 5-HT$_{5A}$ receptor in the startle circuit and behavior of goldfish.

Startle is a common tool for neuropharmacological studies because it offers an easily quantified indicator of neural excitability and is the final common path for multiple modulatory processes (Koch, 1999; Koch and Fendt, 2003). Startle plasticity is commonly studied with the prepulse inhibition (PPI) paradigm, a measure of sensorimotor gating evoked by weak stimuli that attenuate the startle response elicited by subsequent stronger stimuli (Graham, 1975; Hoffman and Ison, 1980; Koch, 1999). Deficits in PPI are associated with several information processing disorders, notably schizophrenia (Braff et al., 2001; Braff, 2010). Importantly, schizophrenic populations also exhibit an abnormality in 5-HT$_{5A}$ coding sequences, making this receptor a potential clinical target (Arias et al., 2001; Iwata et al., 2001; Thomas, 2006).

The Mauthner-cell (M-cell) system of fish presents a unique opportunity to characterize the functionality of 5-HT$_{5A}$ in the context of a vertebrate circuit accessible for *in vivo* electrophysiology. The two reticulospinal M-cells integrate excitatory and inhibitory multimodal inputs; most prominently, a direct, monosynaptic excitation from the auditory vestibular (VIIIth)

nerve (Furukawa and Ishii, 1967; Korn and Faber, 2005). A single action potential (AP) in one M-cell initiates the characteristic startle response, the C-start (Zottoli, 1977; Weiss et al., 2006). Therefore, the M-cells provide the sensorimotor interface of the startle circuit and have proven to be ideally suited to study the mechanisms underlying startle plasticity and sensorimotor gating in goldfish (Neumeister et al., 2008; Medan and Preuss, 2011), African cichlids (Neumeister et al., 2010; Whitaker et al., 2011), and zebrafish (Burgess and Granato, 2007).

The M-cell is innervated by 5-HT projections of at least two types (Gotow et al., 1990; Whitaker et al., 2011); furthermore, Mintz and Korn (1991) demonstrated serotonergic modulation of the presynaptic inhibitory network as well as postsynaptic modulation of the M-cell itself. Importantly, Whitaker et al. (2011) showed that only 5-HT$_5$ and 5-HT$_6$ receptors are expressed in the M-cell. These studies provided the rationale for investigating the functional role of 5-HT$_{5A}$ receptors in the vertebrate startle circuit with complementary electrophysiological and behavioral experiments in goldfish. Our results indicate that 5-HT$_{5A}$ regulates M-cell excitability by modulation of a membrane conductance, which in turn influences the magnitude of sensorimotor gating and behavioral PPI.

Materials and Methods

Subjects. Sixty goldfish (*Carassius auratus*) of either sex, 7–13 cm in standard body length (purchased from Billy Bland Fisheries, Hunting Creek Fisheries, or Ozark Fisheries), were used in the behavior ($n = 28$) and physiology ($n = 32$) experiments. Fish were allowed to acclimate for 3 weeks after transport in rectangular Plexiglas holding tanks (30 × 30 × 60 cm; 95 L). Tanks were supplied with recirculating conditioned water maintained at 18°C. Water was conditioned as described in detail by Szabo et al. (2006). Ambient light was set to a 12 h light/dark photoperiod.

Behavioral experiments. Experiments were conducted in a circular acrylic tank (76 cm diameter, 20 cm water height) mounted on an anti-vibration table to reduce external mechanosensory cues. To minimize visual cues, the top cover and sides of the tank were rendered opaque. Conditioned water circulating through the tank and connecting to an external reservoir was maintained at 18°C. Single goldfish were transferred using a small plastic container from the holding tank into the center of the experimental tank. Animals were given a 10 min acclimation time to the tank before they were injected either for drug or sham (saline) treatment, followed by another 10 min acclimation period before the first experimental trial (see below).

As previously described by Neumeister et al. (2008), ventral views of the freely swimming fish were recorded via a mirror placed below the tank at a 45° angle, using a high-speed video camera (Olympus iSpeed2). Recordings were saved to a hard drive. Two underwater loudspeakers located at opposite sides inside the experimental tank were used to deliver sound stimuli consisting of 200 Hz sound pulses (5 ms duration) created as single-cycle sine waves with Igor Pro software (Wavemetrics) and amplified with a Servo 120 amplifier (Samson). For PPI trials, a nonstartling acoustic pulse (prepulse) ranging from 128.8 to 137.32 dB preceded a startle pulse of 151.93–169.29 dB (SPL relative to 1 μPa in water, which translates to ~62 dB less in air relative to 20 μPa, i.e., relative to the human hearing threshold). The prepulse–pulse interstimulus interval (ISI) was measured from onset of stimuli. ISIs of 50 or 500 ms were used to characterize short- and long-lasting PPI effects. Pulses without preceding prepulses were used to elicit baseline startle responses.

Startle rates (evoked startles/trials) were determined in three different stimulus conditions presented in random order; each fish was exposed to 14 pulse-only trials, five PPI trials with an ISI of 50 ms, and five PPI trials with an ISI of 500 ms. Speakers (left or right) were randomly alternated between each trial, and the time between trials varied from 1 to 8 min to avoid habituation.

Startle escape responses were recorded and visually examined at a time resolution of ±1 ms to determine startle rate and response latency. Re-

sponses with latencies >18 ms were excluded from the analysis (mean of 2.1 trials per fish) because they cannot unambiguously be associated with M-cell activity (Zottoli, 1977). Escapes in response to a prepulse stimulus were also excluded (mean of 3.5 trials per fish). The assessment of invalid trials was done during the experiments and compensated by adding respective trials to the ongoing experiment to reach a consistent number of trials (24).

Behavioral pharmacology. SB-699551 (3-cyclopentyl-N-[2-(dimethylamino)ethyl]-N-[(4′-{[(2-phenylethyl)amino]methyl}-4-biphenylyl)methyl] propanamide dihydrochloride) (Tocris Biosciences), a selective 5-HT$_{5A}$ antagonist (Corbett et al., 2005), was dissolved in saline and administered via intraperitoneal injections in treatment conditions and saline vehicle in control conditions. Fish were briefly removed from the experimental tank for injection; this procedure did not last longer than a few seconds, and the fish typically immediately resumed swimming when released. Volumes injected did not exceed 200 μl. In an initial series of experiments, we used a within-subjects design with a saline control and three different dosages of SB-699551 (0.5, 0.75, and 0.9 mg/kg body weight) in subsequent experimental sessions. Each experimental session was 15–20 d (mean of 16.58 d) apart.

A second series of experiments was conducted with a between-subjects design, wherein subjects randomly received injections either of saline or SB-699551 at the 0.90 mg/kg dosage. Eighteen goldfish were randomly assigned to either the saline or SB-699551 (0.90 mg/kg) treatment condition. Acoustic startle stimuli were presented at three intensities, with a similar range as above; each fish was exposed to 24 pulse-only trials. Speakers (left or right) and stimulus intensity were randomly alternated between each trial. The time between trials varied randomly from 1 to 8 min (to avoid habituation), but the total duration of behavioral testing for each animal was 108 min. The experimenters were blind to the subject's treatment condition during experimentation and analysis.

Electrophysiology. We used previously described *in vivo* surgical and electrophysiological recording techniques (Preuss and Faber, 2003; Medan and Preuss, 2011). Subjects were immersed in ice water for 10–15 min and then treated with topical anesthetic (20% benzocaine gel; Ultradent) at incision sites and pressure points (pin placement) 5 min before surgical procedures. Fish were then placed in the recording chamber, stabilized with one steel pin on each side of the head, and ventilated through the mouth with recirculating, aerated conditioned water at 18°C. The general anesthetic MS-222 was dissolved in the recirculating water at a dosage (20 mg/L) that does not interfere with auditory processing (Palmer and Mensinger, 2004; Cordova and Braun, 2007). The recording chamber was mounted inside an opaque, thin-walled tank filled with temperature controlled (18°C) water covering the fish body up to the midline.

Next, the spinal cord was exposed with a small lateral incision at the caudal midbody. Bipolar electrodes were placed on the unopened spinal cord to transmit low-intensity (5–8 V) electrical stimulation generated by an isolated stimulator (Digitimer). This allowed antidromic activation of the M-cell axons, confirmed by a visible muscular contraction (twitch). Subjects were then injected intramuscularly with D-tubocurarine (1 μg/g body weight; Abbott Laboratories), and a small craniotomy exposed the medulla for intracellular recordings. In anticipation of later experimental drug treatments, an injection needle connected with tubing to a syringe was inserted intramuscularly before placement of recording electrodes.

Antidromic stimulation produces a negative potential in the M-cell axon cap (typically 15–20 mV), which unambiguously identifies the axon hillock and allows intracellular recordings from defined locations along the M-cell soma–dendritic membrane (Furukawa and Ishii, 1967; Faber et al., 1989). Intracellular recording of M-cell responses to sound stimuli were acquired using an Axoprobe-1A amplifier (Molecular Devices) in current-clamp mode with sharp electrodes (3–8 MΩ) filled with 5 M potassium acetate (KAc) or 5 M potassium chloride (KCl$^-$). Recordings were stored online with a Macintosh G5 computer using a data acquisition card (PCI-E; National Instruments) sampling at 25 kHz.

Sound stimuli consisted of single-cycle sound pips (200 Hz) produced by a function generator (Agilent 33210A) connected to a shielded subwoofer (SA-WN250; Sony) located at 30 cm distance to the recording chamber; however, because of transfer loss through the

media of the recording chamber, maximum underwater sound intensity was limited to 147 dB relative to 1 μPa in water. However, these limitations did not hinder physiology assessment of subthreshold prepulse effects because those intensities resemble the prepulse intensities used in the behavioral experiments (Neumeister et al., 2008). Sound stimuli were recorded with a microphone placed 10 cm over the fish's head and stored together with the recordings. A hydrophone (SQ01; Sensor) was used for sound calibration but was removed during experiments.

PPI of the M-cell synaptic response was measured by presenting sound pulses separated by 20, 50, 150, or 500 ms ISIs (as in the study by Medan and Preuss, 2011). The peak amplitude of the postsynaptic potential (PSP) activated by the leading sound pulse (PSP$_{prepulse}$) was compared with the peak amplitude of the PSP activated by the latter sound pulse (PSP$_{pulse}$) to provide a measure of PPI. The PPI effect was calculated as $(100 - \text{PSP}_{pulse}/\text{PSP}_{prepulse} \times 100)$, the implication being that higher percentages reflect greater PPI. Average values were computed from measures in 5–10 traces and were used for analysis.

To examine the effect of 5-HT$_{5A}$ antagonists on membrane properties previously studied in the M-cell, such as AP thresholds, input resistance, and linearity (Neumeister et al., 2008; Medan and Preuss, 2011), we injected current ramps via a second intrasomatic electrode (KAc; 3–5 MΩ) while maintaining the voltage recordings. A function generator (model 39; Wavetek) was used to regulate current injection, producing a positive current ramp (0–200 nA/20 ms). A compensation circuit built in the Axoprobe-1A amplifier eliminated crosstalk between the electrodes. Current–voltage (I/V) relationships were measured without sensory stimulation or with an auditory prepulse (200 Hz, 147 dB) preceding current injection by 20, 50, 150, or 500 ms.

After assessment of baseline conditions, subjects were injected with 5-HT$_{5A}$ antagonists. In experiments with SB-699551, the drug was dissolved in saline at a dosage of 0.90 mg/kg body weight, and measures taken in the baseline condition were repeated 10–30 min after injection. Resting membrane potential (RMP) was continuously monitored to ensure stable recording conditions and/or possible effects of the drug on this parameter. A typical experiment lasted 3–4 h. In another subset of electrophysiology experiments, we used an alternative selective 5-HT$_{5A}$ antagonist, A-843277 (*N*-(2,6-dimethoxybenzyl)-*N′*[4-(4-fluorophenyl) thiazol-2-yl]guanidine), which was kindly provided by R. L. Gannon (personal communication; Gannon et al., 2009). As per the instructions provided, and, similar to the method reported by Kassai et al. (2012), the drug was dissolved in distilled water with 15 μl of Tween 80 (Sigma), for a final dosage concentration of 10 mg/kg body weight, as was applied by Gannon et al. (2009) and Kassai et al. (2012). Experiments with A-843277 were otherwise identical to those in which SB-699551 was administered, because the intent was to compare the consistency of the effect of each antagonist.

All experiments were conducted according to the guidelines and approved protocols of the Hunter College (City University of New York) Institutional Animal Care and Use Committee.

Statistical analyses. Data were analyzed with JMP 8.0.2 (SAS Institute), and figures were created in GraphPad Prism (version 5.0) or Igor Pro (version 5.03; Wavemetrics). Data presented in figures describe mean values, and error bars illustrate SEM. D'Agostino's and Pearson's omnibus normality tests were used to confirm that datasets met assumptions of normality. Given the parameters of our data, we tested inferential statistical hypotheses with generalized linear mixed models (GLMMs). The GLMM is the appropriate statistical model for this dataset because it allows comparison of continuous conditions (e.g., ISI), can accommodate unequal sample sizes, and allows inferential tests of two-way interactions and effects. In all analyses, subjects were treated as random effects (thus, repeated measures) and stimulus (no prepulse, ISI$_{20 ms}$, ISI$_{50 ms}$, ISI$_{150 ms}$, ISI$_{500 ms}$) and dosage (saline, 0.50, 0.75, 0.90 mg/kg body weight) conditions were treated as fixed effects. Dependent variables tested in these models included startle probability, threshold voltage, threshold current, and input resistance. Note that the peak magnitude of PSPs and the latency to peak magnitude of the PSP were the only effects not tested in a GLMM because those tests did not need to consider multiple factors

and levels; accordingly, simple matched *t* tests were applied for these direct tests.

Results
Behavior
The initial behavioral experiments tested the effect of three different dosages (0.50, 0.75, 0.90 mg/kg body weight) of the 5-HT$_{5A}$ antagonist SB-699551 on the acoustic startle rate of fish in three stimulus conditions: with no prepulse or with prepulses at ISIs of 50 or 500 ms. The results of those experiments, presented in Figure 1A, showed a decline in mean startle rates that was most pronounced in prepulse trials with the two highest dosages of the 5-HT$_{5A}$ antagonist. Specifically, we found that startle rates in the ISI$_{50 ms}$ and ISI$_{500 ms}$ stimulus conditions were most strongly affected by the drug at the 0.75 mg/kg (ISI$_{50 ms}$, 74.07 $\pm$ 22.07% reduction; ISI$_{500 ms}$, 80 $\pm$ 15.28% reduction) and 0.90 mg/kg (ISI$_{50 ms}$, 87.5 $\pm$ 15.28% reduction; ISI$_{500 ms}$, 70 $\pm$ 24.94% reduction) dosages relative to saline controls. Startle rates in the no-prepulse stimulus condition were less sensitive to drug treatment (Fig. 1A, black line; maximum dosage effect, 14.01% reduction at 0.90 mg/kg dosage) than startle rates in prepulse conditions (Fig. 1A). We tested the significance of dosage and stimulus condition effects on startle probability in a GLMM. Our analysis identified significant main effects of antagonist dosage ($F_{(3,99)} = 11.78$, $n = 10$, $p < 0.0001$) and stimulus ($F_{(8,99)} = 13.9494$, $n = 10$, $p < 0.0001$) conditions on startle probability. *Post hoc* analyses (Tukey's HSD) found no significant effects of dosage conditions on startle probability in no-prepulse stimulus conditions, but startle rates were significantly reduced in prepulse trials for ISI$_{50 ms}$ at the 0.90 mg/kg dosage ($p = 0.0214$) and for ISI$_{500 ms}$ at both the 0.75 mg/g ($p = 0.0071$) and 0.90 mg/kg ($p = 0.0316$) dosages compared with saline controls (Fig. 1A). The magnitude of PPI is typically quantified by comparing startle probability in no-prepulse trials with prepulse trials for the same dosage. Figure 1B plots this quantification of PPI across dosage conditions to illustrate two important effects. First, treatment with the antagonist seemingly enhanced PPI, particularly for ISI$_{500 ms}$ (Fig. 1B, light gray line). Second, these facilitations of PPI also produced a convergence of PPI magnitude for ISI$_{50 ms}$ and ISI$_{500 ms}$ stimulus conditions, essentially eliminating ISI dependencies. This lack of ISI dependency might indicate a drug-induced saturation of PPI. Alternatively, the apparent facilitation of PPI could indicate a generalized reduction of excitability in the startle circuit that is added to the inhibition evoked by the prepulse; indeed, the 14.01% reduction in startle responsiveness in pulse-only conditions (Fig. 1A, black line, saline vs 0.75 and 0.90 mg/kg dosages) provides some support for this interpretation.

To directly test the effect of the 5-HT$_{5A}$ antagonist on startle sensitivity independent of the prepulse inhibitory network, we tested subjects ($n = 18$) in a between-groups design using startle stimuli in the same intensity range as above. We found that subjects in the SB-699551 (0.90 mg/kg) group (Fig. 1C, gray line) had significantly lower startle rates than subjects in the saline-injected group (Fig. 1C, black line) ($F_{(1,48)} = 13.13$, $p = 0.0007$, $n = 18$), but neither stimulus intensity ($F_{(2,48)} = 1.022$, $p = 0.3675$, $n = 18$) nor the interaction of drug $\times$ intensity ($F_{(2,48)} = 0.3804$, $p = 0.6856$, $n = 18$) had any significant effect on startle probability. The general depression of the startle stimulus–response curve in the SB-699551 condition indicates that the 5-HT$_{5A}$ antagonist reduced startle rates over the whole range of stimulus intensities used. Additionally, an analysis of startle rates across trials indicated that there was no significant change in startle rate over the course of the experiment ($F_{(1,46)} = 1.0163$, $p = 0.4432$). Thus, the
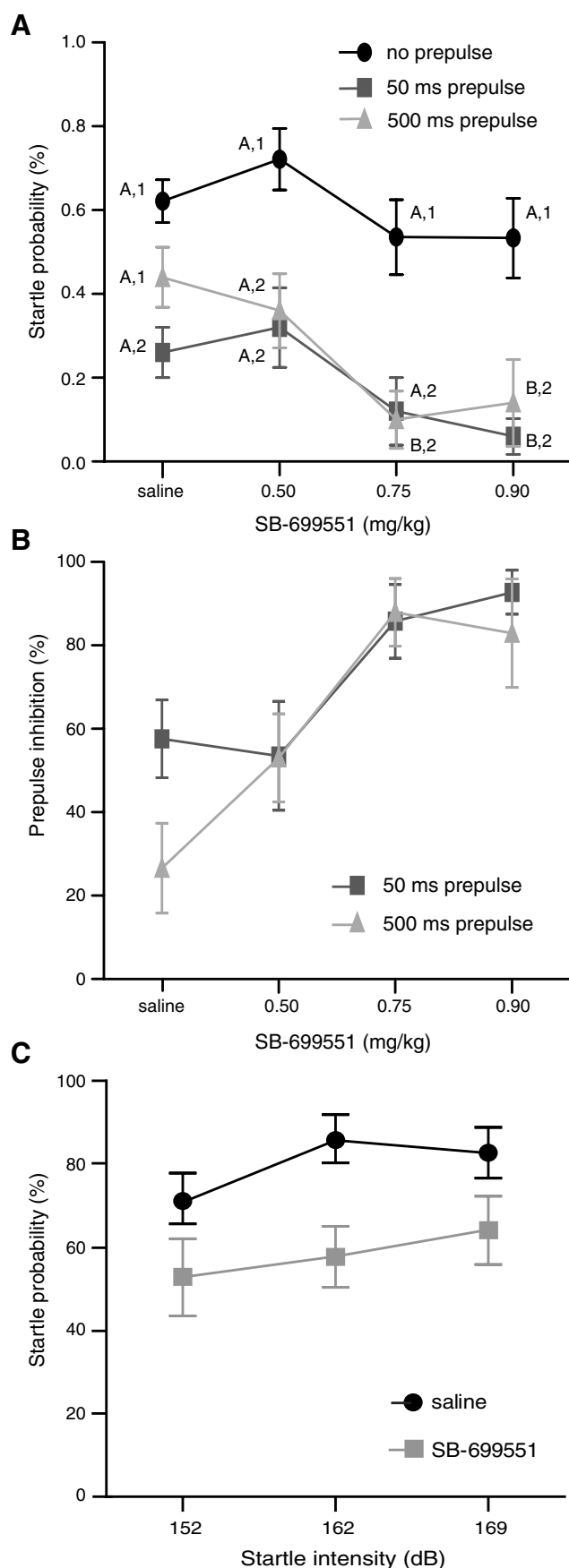
available data indicate that the drug effectively and consistently reduced startle over the 108 min of behavioral testing.

Physiology

The goal of the physiology experiments was to identify the effector mechanisms that the 5-HT$_{5A}$ antagonist acted on to reduce startle sensitivity in behavioral tests. Given that the behavioral results indicated a strong effect of SB-699551 at 0.90 mg/kg and the challenges of *in vivo* electrophysiology, all physiological experiments with SB-699551 were conducted at that dosage. An additional 5-HT$_{5A}$-selective antagonist, A-843277 (10 mg/kg body weight), was also applied in some physiological experiments to confirm that the effects observed were consistent and not specific to a distinct antagonist.

5-HT$_{5A}$ antagonist attenuates synaptic response

We first recorded the synaptic response of the M-cell to sound pips (without prepulse) before and after drug application. We found that SB-699551 reduced sound-evoked PSPs in the M-cell (Fig. 2A). To quantify this effect, we measured the peak amplitude of M-cell PSPs (control, $n = 14$, mean of 5.98 ± 0.63 mV) and found a $26.41 \pm 3.98\%$ decrease in peak depolarization after treatment with SB-699551 (paired t test, $n = 14$, $t = 4.176$, $p = 0.0011$; Fig. 2B). However, the latency to peak depolarization from the onset of sound (latency$_{control}$ = 4.24 ± 0.14 ms, $n = 14$) was unaffected by treatment with SB-699551 (paired t test, $n = 14$, $p = 0.2342$). These findings indicate a generalized drug-induced reduction in sound-evoked excitation that did not affect the temporal characteristics of the sound-evoked PSP.

Next, we administered a different 5-HT$_{5A}$-selective antagonist, A-843277, to test whether the effects produced by the selective antagonist SB-699551 could be reproduced by an alternative selective 5-HT$_{5A}$ antagonist. The effects of A-843277 on the sound-evoked PSP were, in fact, similar to the effects of SB-699551 (Fig. 2A, compare black trace with gray trace; C, compare black trace with gray trace); that is, A-843277 caused a significant reduction ($17.52 \pm 6.24\%$ reduction in peak magnitude; paired t test, $n = 7$, $t = 2.629$, $p = 0.03$) in the peak amplitude of sound-evoked PSPs (PSP$_{control}$ = 6.203 ± 0.59 mV; PSP$_{A-843277}$ = 5.26 ± 0.78 mV; Fig. 2D, black vs gray bars). As with SB-699551, the latency to peak depolarization from the onset of sound stimuli was unaffected (paired t test, $n = 7$, $t = 0.1586$, $p = 0.1586$) by treatment with A-843277 (latency$_{control}$ = 4.76 ± 0.18 ms, $n = 7$; latency$_{A-843277}$ = 5.35 ± 0.59 ms, $n = 7$).

We then asked how 5-HT$_{5A}$ antagonists affected synaptic PPI by measuring the amplitude of M-cell PSPs after a preceding sound pulse at four ISIs (20, 50, 150, 500 ms). Figure 3A shows sample recordings at ISI 50 ms illustrating that a prepulse decreased the overall magnitude of the pulse PSP (black trace vs red trace). Repeating the experiment 10–25 min after drug application showed, as expected, a reduction in the PSP$_{pulse}$ compared

←

prepulse (black) and with preceding acoustic prepulse stimuli at two ISIs (gray lines). Different letters and numbers (e.g., A,1 or B,2) indicate significant differences among drug (letters) and stimulus (numbers) conditions, respectively (*post hoc* Tukey's HSD, $p < 0.05$). **B**, Plots of the calculated mean $\pm$ SEM PPI effect for ISI$_{50 ms}$ (dark gray) and ISI$_{500 ms}$ (light gray) across dosages ($n = 10$). Note that the PPI effect was calculated from the data shown in **A**. **C**, Mean $\pm$ SEM startle rates in response to pulse-only (no prepulse) acoustic stimuli for naive subjects in saline ($n = 9$, black line) and SB-699551 ($n = 9$, gray line) treatment conditions for three different startle stimulus intensities (x-axis, decibel relative to 1 μPa in water). Note that there was no significant difference across stimulus intensities, but treatment conditions (black vs blue lines) were significantly different (GLMM, $p = 0.0007$).
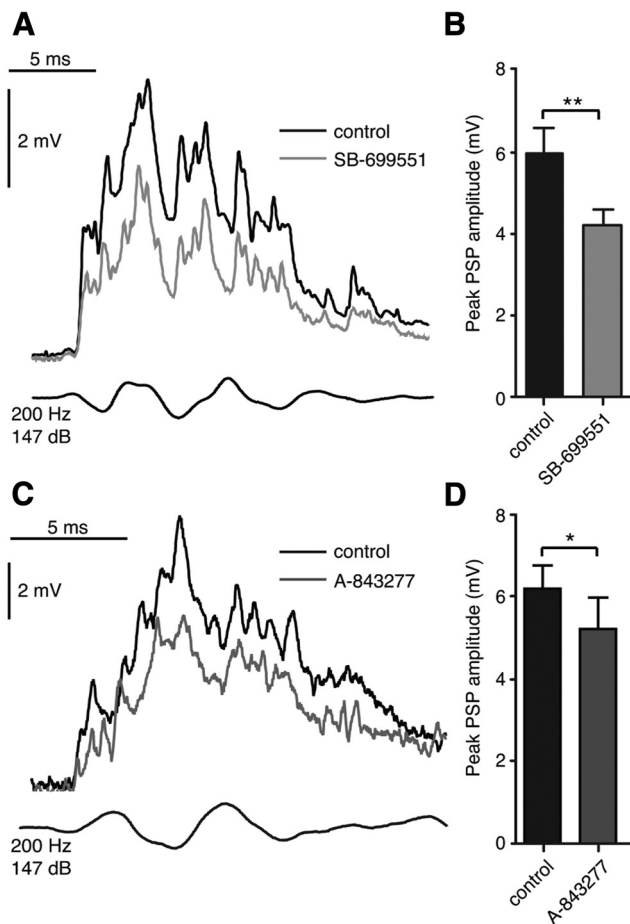
Figure 1. The 5-HT$_{5A}$ antagonist SB-699551 reduces startle rate during PPI. **A**, Mean $\pm$ SEM startle rates ($n = 10$) at different drug dosages (x-axis) to startling sound stimuli with no

Figure 2. 5-HT$_{5A}$ antagonists attenuate the M-cell synaptic sound response. **A**, Exemplar traces (KAc electrodes) showing sound-evoked PSPs recorded in the M-cell before (black) and after (gray) treatment with the 5-HT$_{5A}$ antagonist SB-699551. Bottom trace indicates sound stimuli (200 Hz, pips at 147 dB relative to 1 μPa in water). **B**, Plots of mean $\pm$ SEM peak amplitudes of sound-evoked PSPs ($n = 14$) for control and SB-699551 treatment. Paired t test, **$p = 0.0011$. **C**, Exemplar traces, as in **A** (KAc electrodes), but here subjects were treated with the 5-HT$_{5A}$ antagonist A-843277 (10 mg/kg body weight). Black trace shows control conditions, and gray trace shows sound responses after treatment with A-843277. **D**, Plots of mean $\pm$ SEM peak amplitudes of sound-evoked PSPs ($n = 7$) for control and A-843277 treatment conditions. Paired t test, *$p = 0.03$. Note that both antagonists produced similar effects.

with nondrug controls (Fig. 3A, black vs blue trace), with an added attenuation of the PSP after a prepulse (Fig. 3A, black and blue vs red traces). In other words, with drug treatment, the PPI effect is superimposed onto a tonic inhibition (Fig. 3A, gray double-arrowhead line); however, the PPI effect itself appears essentially unchanged (Fig. 3A, brackets). To test this notion, we compared the PPI effect ($100 - \text{PSP}_{\text{prepulse}}/\text{PSP}_{\text{pulse}} \times 100$) on the PSP peak amplitude between control and drug conditions at different ISIs. The results showed that the duration of ISIs determined the magnitude of prepulse–pulse attenuation ($F_{(3,32)} = 35.59$, $p < 0.0001$, $n = 9$), but SB-699551 caused no significant change in the PPI effect itself ($F_{(1,32)} = 0.95$, $p = 0.3367$, $n = 9$; Fig. 3B). Furthermore, we found no significant interaction between ISI and drug treatment factors ($F_{(3,32)} = 0.59$, $p = 0.6270$, $n = 9$). Importantly, this measure (percentage PPI) reflects the reduction in $\text{PSP}_{\text{pulse}}$ relative to $\text{PSP}_{\text{prepulse}}$ in the same treatment condition, meaning that the relative consistency of prepulse–pulse relationships are tested but the context in which they occur (i.e., significantly reduced excitation) are not. We replicated these stimulus conditions with application of A-843277 and found, as

before, similar results (Fig. 3C). That is, whereas ISI is a significant determinant of percentage PPI ($F_{(3,24)} = 51.58$, $p < 0.0001$, $n = 7$), neither A-843277 ($F_{(1,24)} = 0.06$, $p = 0.6224$, $n = 7$) nor the interaction of ISI and A-843277 ($F_{(3,24)} = 0.16$, $p = 0.9208$, $n = 7$) caused any significant change in PPI. Together, these results indicate that 5-HT$_{5A}$ antagonists reduced the synaptic response to sound pips in the M-cell but do not affect synaptic PPI.

Effects of 5-HT$_{5A}$ on M-cell membrane properties
As noted, we showed previously that the 5-HT$_{5A}$ receptor is expressed in the M-cell (Whitaker et al., 2011). Hypothesizing that the receptor is functional, we next asked whether SB-699551 reduces the synaptic response through a postsynaptic mechanism. To test this, we measured drug- and PPI-evoked changes in M-cell input resistance by injecting a current ramp into the M-cell lateral proximal dendrite while recording membrane voltage with a second electrode in the soma (see Materials and Methods). The rationale of using a current ramp was to assess drug effects on different M-cell properties (e.g., threshold current and voltage-dependent conductances) over the full range of membrane depolarizations in a standardized manner (Neumeister et al., 2008). Figure 4A shows sample recordings of such an experiment in different stimulus conditions before and after drug treatment. The M-cell exhibits a well-characterized (Faber and Korn, 1986; Neumeister et al., 2008) membrane nonlinearity that dynamically increases resistance (thus, excitability) when membrane depolarization exceeds 5 mV (Faber and Korn, 1986; Neumeister et al., 2008). This nonlinearity can be characterized by measuring initial-state input resistance (slope 1) defined as the I/V slope 0–2 ms from onset of current injection (Fig. 4B) and at a depolarized-state input resistance, slope 2 (I/V slope measured 1–3 ms before the onset of the AP; Fig. 4B). Neumeister et al. (2008) and Medan and Preuss (2011) showed that prepulse stimuli reduce input resistance differently in the initial state and depolarized state, providing two distinct cellular mechanisms that contribute to PPI (Fig. 4B, black vs red plots; Neumeister et al., 2008; Medan and Preuss, 2011). Accordingly, we analyzed the putative effect of SB-699551 on initial-state and depolarized-state input resistance after acoustic prepulses at four distinct lead times (20, 50, 150, 500 ms).

Our results indicate that prepulse stimuli and the 5-HT$_{5A}$ antagonist activate independent but additive postsynaptic mechanisms that contribute to startle inhibition. Namely, we identified significant variability of slope 1 across different prepulse–pulse ISIs ($F_{(4,81)} = 15.11$, $p < 0.001$; Fig. 4C, no-prepulse vs ISIs, compare numbers) and drug treatment ($F_{(1,81)} = 32.81$, $p < 0.0001$; Fig. 4C, black vs blue lines, compare letters) conditions. Post hoc tests revealed that input resistance was significantly reduced for ISI$_{20 \text{ ms}}$ ($p < 0.0001$), ISI$_{50 \text{ ms}}$ ($p < 0.0478$), and ISI$_{150 \text{ ms}}$ ($p < 0.0094$) stimulus conditions relative to no-prepulse controls. Post hoc tests also revealed that treatment with the antagonist caused a significant reduction in input resistance ($t = -5.728$, $p < 0.0001$), but there was no significant interaction between the effects of prepulses and the effect of the drug ($F_{(4,81)} = 0.2054$, $p = 0.9347$). These findings distinguish between a cellular mechanism that contributes to short-lasting (20–150 ms) PPI and a general inhibitory shunt (see below) of M-cell excitability after treatment with the antagonist. Importantly, these effects are cumulative, i.e., the initial-state membrane is least excitable in PPI conditions after treatment with the antagonist.

We identified a similar convergence of inhibitory mechanisms active in the depolarized membrane, i.e., a significant reduction in slope 2 ($F_{(4,81)} = 7.181$, $p < 0.0001$; Fig. 4D, no-prepulse vs ISIs) for all ISIs (ISI$_{20 \text{ ms}}$, $p < 0.0001$; ISI$_{50 \text{ ms}}$, $p = 0.0004$; ISI$_{150 \text{ ms}}$,
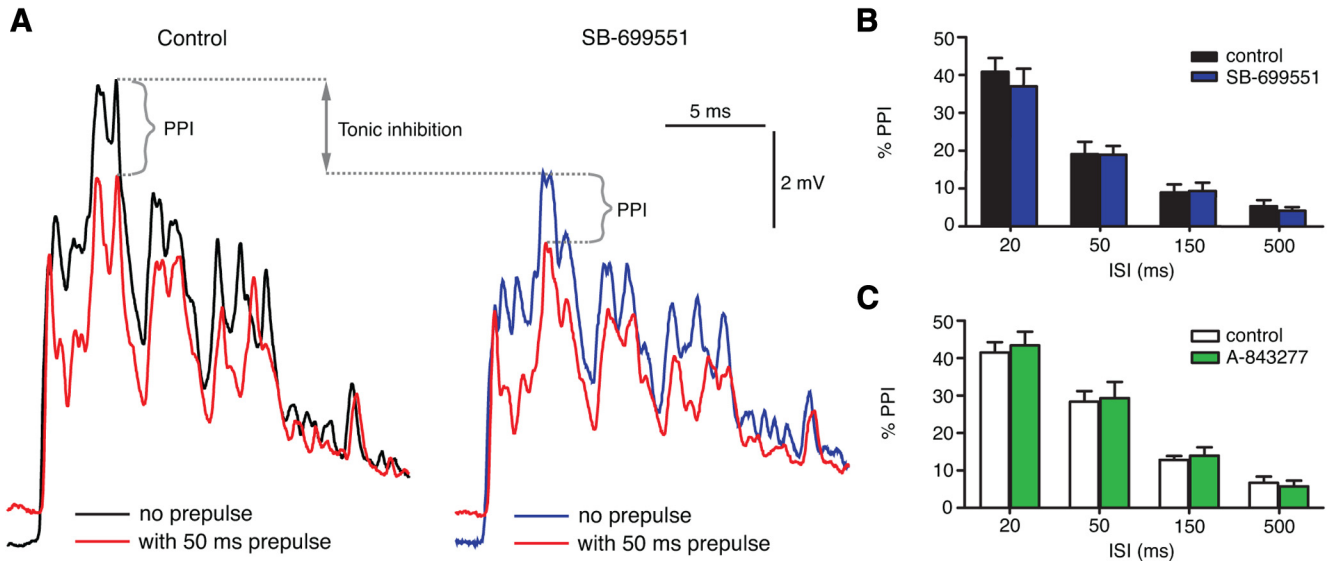
A

Figure 3. Convergence of discrete inhibitory mechanisms. **A**, Exemplar traces (KAc electrodes) showing the sound-evoked PSPs with no prepulse (black) and with prepulse (ISI$_{50\,ms}$, red) in drug control (left traces) and SB-699551 conditions (right traces). The sound stimulus was identical in all traces (200 Hz, pips at 147 dB relative to 1 μPa in water). Note that prepulse-evoked inhibition (indicated in brackets) is similar in control and drug conditions but is superimposed (indicated by double-arrowed line) on a tonic inhibition after treatment with SB-699551. **B**, Plots of mean ± SEM synaptic PPI effect ($n = 9$) (see **A**) at varying ISIs in control (black bars) and SB-699551 (blue bars) treatment conditions. ISI is a significant determinant of PPI intensity (2-way repeated-measures ANOVA, $p < 0.0001$), but SB-699551 caused no significant change in the PPI effect itself ($p = 0.3367$), nor was there any interaction between drug and ISI conditions ($p = 0.6270$). **C**, Plots of mean ± SEM synaptic PPI effect ($n = 7$), as in **B**, at varying ISIs in control (white bars) and A-843277 (green bars) treatment conditions. As in **B**, ISI is a significant determinant of PPI intensity (2-way repeated-measures ANOVA, $p < 0.0001$), but there was no significant change in PPI intensity attributable to drug treatment ($p = 0.6224$) or the interaction of ISI and drug treatment ($p = 0.9208$).

$p = 0.0105$; ISI$_{500\,ms}$, $p = 0.0098$) relative to no-prepulse controls and drug treatment ($F_{(1,81)} = 31.644$, $p < 0.0001$; Fig. 4D, black vs blue lines; *post hoc* $t = -5.625$, $p < 0.0001$). As for slope 1, there was no significant interaction between drug treatment and stimulus condition effects ($F_{(4,81)} = 1.8199$, $p = 0.133$).

SB-699551 had no effect on RMP (RMP$_{control}$ = -80.91 ± 0.95 mV, $n = 13$; RMP$_{SB-699551}$ = -81.61 ± 1.414 mV, $n = 9$; Student's $t = 0.4223$, $p = 0.676$). RMP was similarly unaffected by treatment with A-843277 (RMP$_{control}$ = -82.44 ± 1.09 mV; RMP$_{A-843277}$ = -80.74 ± 1.83 mV; paired t test, $n = 7$, $t = 0.9212$, $p = 0.3925$). Consistent with the observed decrease in input resistance, the drug increased threshold current indicated by the observation that current injections (limited to 200 nA by the amplifier) elicited APs only in three of nine fish tested after drug application.

To confirm these results with parallel methods, we compared the amplitude of antidromically evoked M-cell APs after treatment with both 5-HT$_{5A}$ antagonists. Because the M-cell membrane is unexcitable (i.e., non-regenerative), the magnitude of a passively conducted AP provides an indirect measure of input resistance. We found that both selective 5-HT$_{5A}$ antagonists caused a reduction in the peak amplitude of M-cells APs [SB-699551, 10.93 ± 3.41% reduction (Fig. 5A); A-843277, 10.94 ± 1.41% reduction (Fig. 5C)]. These reductions were significant after treatment with SB-695551 (AP$_{control}$ = 33.39 ± 2.46 mV, AP$_{drug}$ = 29.87 ± 2.78 mV; paired t test, $n = 6$, $t = 3.608$, $p = 0.0154$; Fig. 5B) and with A-843277 (AP$_{control}$ = 35.2984 ± 1.55 mV, AP$_{drug}$ = 31.4414 ± 1.53 mV; paired t test, $n = 5$, $t = 7.7566$, $p = 0.0015$; Fig. 5D). We also compared the effects of the drugs on the width (duration) of APs, measured at one-third of peak depolarization. Neither SB-699551 nor A-843277 produced any significant change in AP duration (SB-699551, paired t test, $n = 6$, $t = 0.1253$, $p = 0.9052$; A-843277, paired t test, $n = 5$, $t = 0.1625$, $p = 0.8788$). In summary, these findings provide additional confirmation that antagonizing the 5-HT$_{5A}$ receptor produces

a depression of postsynaptic excitability. Additionally, the consistency of these effects provides evidence that each antagonist acts selectively on the 5-HT$_{5A}$ receptor.

SB-699551 enhances Cl$^-$ conductance

Tonic inhibition in the M-cell is linked to changes in Cl$^-$ conductance (Korn et al., 1987; Hatta and Korn, 1999; for review, see Korn and Faber, 2005). Accordingly, in these experiments, we tested whether changes in Cl$^-$ conductance were related to the tonic changes in M-cell excitability we observed in previous experiments (see above). Because the M-cell RMP is near the Cl$^-$ equilibrium potential, changes in Cl$^-$ conductance do not produce changes in M-cell membrane potential when recordings are made with KAc solutions, as were used in all previous experiments. However, intracellular recordings made with KCl recording solutions can reveal Cl$^-$ currents as frank membrane depolarizations by altering the local Cl$^-$ concentration and thereby driving force (Fukami et al., 1965; Diamond and Huxley, 1968; Diamond et al., 1973). Consequently, if the reduced excitability we found in previous experiments was driven by an increase in Cl$^-$ conductance, then the 5-HT$_{5A}$ antagonist should evoke an increase in depolarization with KCl recording solution.

We tested this notion by recording intracellular responses to sound stimuli in control and drug conditions as in previous experiments but using electrodes filled with a KCl (5 M) recording solution. The M-cell PSPs include purely excitatory and mixed excitatory/inhibitory components that can be dissected by the time course of the response (Szabo et al., 2006; Weiss et al., 2009). Whereas within 5 ms of the onset of sound stimuli the M-cell receives only electrical and chemical excitatory inputs (Fig. 6A, EPSP), the latter part of the response (Fig. 6A, PSP) integrates mixed excitatory and inhibitory inputs from associated feedforward circuits (Pereda et al., 1994; for review, see Korn and Faber, 2005). Accordingly, we analyzed the peak response to sound stimuli at those two intervals. Our results show that the EPSP and
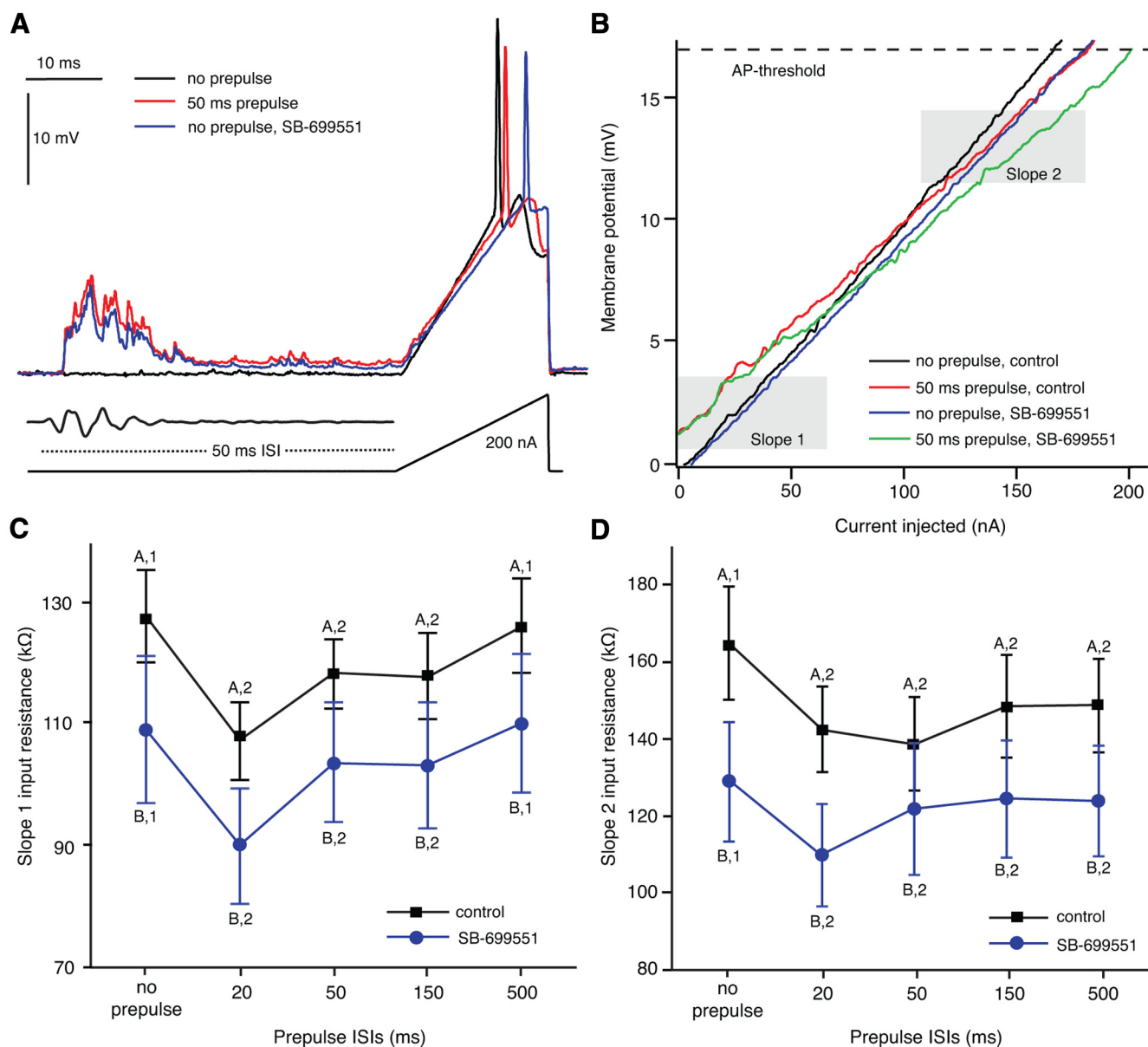
Figure 4. 5-HT$_{5A}$ antagonist evokes postsynaptic reduction in M-cell input resistance. **A**, At top, voltage traces recorded during current injection experiments in control conditions with no prepulse (black), with 50 ms prepulse (red), and with 50 ms prepulse after treatment with SB-699551 (blue). Middle trace shows sound stimulus used for prepulse. Bottom trace shows time course of current injection. **B**, I/V traces show M-cell depolarization during current injection with no prepulse (black) and 50 ms prepulse (red) in control conditions and no prepulse (blue) and with 50 ms prepulse (green) after SB-699551 treatment. The depicted range shows depolarization from RMP to AP threshold (dashed line). Slope 1 and slope 2 (gray boxes) indicate where linear fits were applied to I/V plots to quantify slope (input resistance). **C**, Plots of mean ± SEM input resistance for the initial state (slope 1) of M-cell depolarization (control, $n = 12$, black line; SB-699551, $n = 9$, blue line) with no prepulse and prepulses at varying ISIs in drug control and SB-699551 treatment conditions. Letters and numbers indicate significant differences (GLMM, post hoc, $\alpha = 0.05$) between stimulus conditions (numbers) and drug treatment (letters), respectively. **D**, Plots of mean ± SEM input resistance for the depolarized-state M-cell (control, $n = 12$, black line; SB-699551, $n = 9$, blue line) during PPI and drug treatment conditions. Letters and numbers (e.g., A,1, B,2) indicate significant differences (post hoc, $\alpha = 0.05$) between stimulus (numbers) and treatment (letters) conditions as in **C**.

PSP components of the sound response were equally enhanced by treatment with SB-699551 (Fig. 6A).

Within 5 ms of stimulus onset, we found a significant increase in depolarization after treatment with SB-699551 (Fig. 6B; paired t test, $n = 9$; $t = 3.583$, $p = 0.0089$). Similarly, peak responses >5 ms from stimulus onset showed a significant increase in depolarization (Fig. 6C; paired t test, $n = 9$, $t = 4.062$, $p = 0.0048$). The fact that the 5-HT$_{5A}$ antagonist increased sound-evoked depolarization without changing the time course of the response suggests an underlying tonic enhancement of Cl$^-$ conductance. However, we also considered that the antagonist could produce a conductance change associated with inhibitory networks. Changes in

inhibitory inputs should be apparent in the latter components of the PSP that are not present in the initial EPSP. To test this, we compared the percentage change in EPSPs to PSPs after treatment with SB-699551 but found no significant difference in the effect of the drug over the time course of the sound response (Fig. 6D; paired t test, $n = 9$, $t = 0.9241$, $p = 0.3825$). Together, these results consistently suggest that the 5-HT$_{5A}$ antagonist produces a tonic increase in M-cell Cl$^-$ conductance.

Discussion

The aim of this study was to determine the functional contribution of the 5-HT$_{5A}$ receptor in startle plasticity and sensorimotor
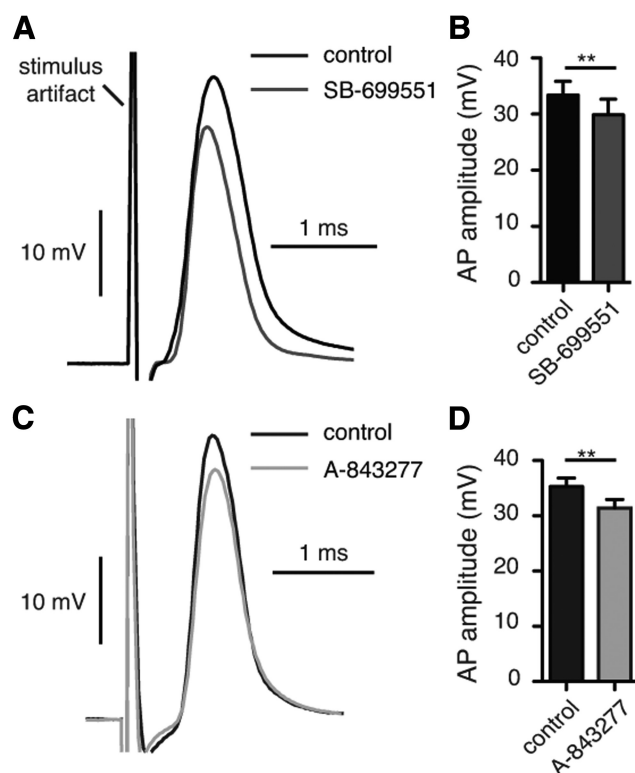
Figure 5. 5-HT$_{5A}$ antagonists reduce the amplitude of M-cell APs. *A*, Traces show an antidromically evoked AP recorded in the soma in control (black trace) and SB-699551 (gray trace) treatment conditions. Recordings were made with KAc electrodes. Note that the recording electrode was not moved before/after drug application. *B*, Plots of mean ± SEM peak depolarization of APs in control and SB-699551 treatment conditions ($n = 6$, paired t test, **$p = 0.0154$). *C*, Traces show antidromically evoked APs in control conditions (black trace) and after treatment with A-843277 (gray trace). Recordings made with KAc electrodes. Note that the recording electrode was not moved before/after drug application. *D*, Plots of mean ± SEM peak depolarization of APs in control and A-843277 treatment conditions ($n = 5$, paired t test, **$p = 0.0015$). Recordings made with KAc electrodes.

gating. Our methodology linked the effect of a selective 5-HT$_{5A}$ antagonist on startle behavior to the underlying neural circuit that controls the behavioral response. Here we report the two main conclusions that can be drawn from our findings and follow with more detailed examination of the evidence in favor of each. First, the 5-HT$_{5A}$ receptor regulates excitability of the startle circuit through a modulation of input resistance, likely through a Cl$^-$ current. Second, antagonizing the 5-HT$_{5A}$ receptor leads to a reduction in startle rate during behavioral PPI (i.e., to an apparent increase in PPI); however, our electrophysiological experiments demonstrate that this is attributable to an additive interaction of drug-induced intrinsic and PPI-induced extrinsic inhibitory mechanisms. We believe these findings are important and of broad interest because they provide a new perspective on the modulation of PPI by intrinsic versus extrinsic factors, an ongoing controversy in the field of sensorimotor gating (see below).

Effects of SB-699551 on the M-cell
The significant reductions in M-cell input resistance after treatments with two distinct 5-HT$_{5A}$ antagonists (Figs. 4, 5) offer independent evidence that the 5-HT$_{5A}$ receptor regulates intrinsic excitability of the M-cell, the decision-making neuron of the startle circuit. Consistent with this, we found significant reductions in the magnitude of sound-evoked M-cell PSPs (Fig. 2) and an attenuation of startle responsiveness. The 5-HT$_{5A}$ receptor
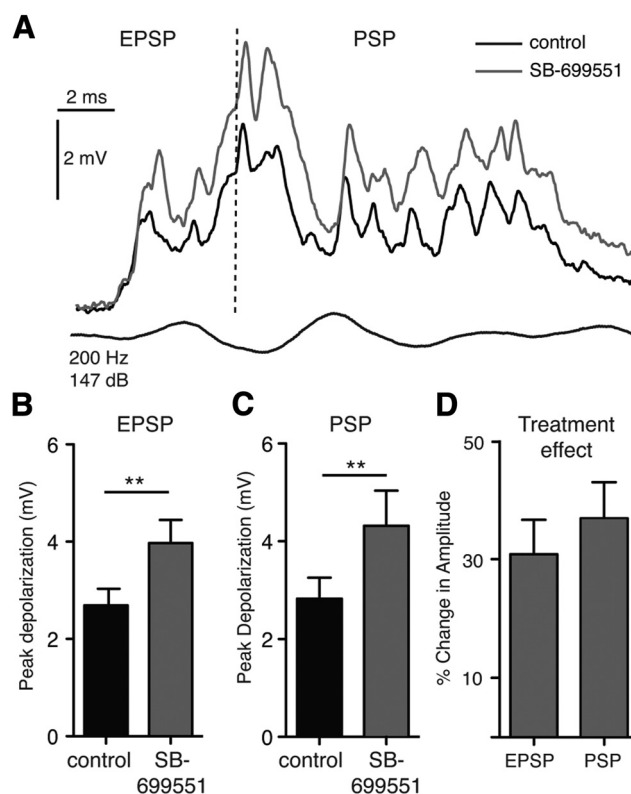

Figure 6. 5-HT$_{5A}$ antagonist increases Cl$^-$ conductance. *A*, Sample traces showing M-cell sound responses recorded with KCl$^-$ (5 M) electrodes. Note that an enhancement of depolarization in these conditions reflects an increase in outward Cl$^-$ conductance attributable to Cl$^-$ loading of the cell (see Results). Black trace shows a recording in control conditions, whereas the gray trace shows a recording after treatment with SB-699551. Dotted line indicates 5 ms latency after stimulus onset; to the left, the sound response can be interpreted as a pure EPSP (i.e., only excitatory components), whereas to the right of the line the response is a mixed EPSP/IPSP. *B*, Plots of mean ± SEM peak depolarization ($n = 9$) (KCl electrodes) of the EPSP; that is, the sound response within <5 ms of stimulus onset. Black bar plots control conditions and gray bar indicates measures after treatment with SB-699551. *C*, Plots of mean ± SEM peak depolarization ($n = 9$) (KCl electrodes) of the sound-evoked PSP >5 ms after stimulus onset. Black bar plots control conditions and gray bar indicates measures after treatment with SB-699551. *D*, Plots of mean ± SEM percentage change ($n = 9$) in sound-evoked depolarization (KCl electrodes) during the initial (EPSP) and latter (PSP) components of the sound response after treatment with SB-699551. Note that there was no significant difference in the effect of the drug across the time course of the response (paired t test, $p = 0.3825$).

was known to be expressed in the M-cell (Whitaker et al., 2011), but our current findings confirm that this receptor is functional and plays an important role in modulating startle responsiveness in goldfish. These results are consistent with past studies of serotonergic modulation in the M-cell system and other startle circuits. Mintz and Korn (1991) found that 5-HT modulates a voltage-dependent conductance in the M-cell. Similarly, 5-HT increases input resistance in the lateral-giant escape neurons of the crayfish (Antonsen and Edwards, 2007). Thus, broadly, 5-HT plays an important role in modulating the excitability of startle-escape circuits and behavior in both vertebrates and invertebrates.

Our results show that a 5-HT$_{5A}$ antagonist decreases M-cell membrane resistance by modulating a M-cell membrane conductance. The effects of SB-699551 were almost equally strong in a membrane close to RMP and close to threshold (Fig. 4), suggesting that the affected conductance shows no voltage dependence within this physiological range of membrane depolarization. Previous studies of the 5-HT$_{5A}$ receptor (Francken et al., 1998; Hurley et al., 1998; Thomas et al., 2000; Noda et al., 2003, 2004) indicate that this recep-

tor is negatively coupled to (i.e., suppresses) adenylyl cyclase formation, which in turn suppresses the cAMP second-messenger system. In the M-cell, accumulation of cAMP enhances glycine-mediated inhibitory Cl$^-$ currents (Wolszon and Faber, 1989) without corresponding changes in RMP, as observed in the present study. Indeed, our results did show an apparent activation of a Cl$^-$ conductance with SB-699551 treatment (Fig. 6) and thus provide an important step in identifying the underlying mechanism(s) through which 5-HT regulates M-cell excitability. However, electrophysiological studies in *ex vivo* preparations have also linked the 5-HT$_{5A}$ receptor to an inward-rectifying K$^+$ current (Noda et al., 2004; Goodfellow et al., 2012). Indeed, in the M-cell, a membrane nonlinearity, linked to an inward rectifier, dynamically increases input resistance during depolarization, and the elimination of this nonlinearity by a prepulse mediates PPI (Faber and Korn, 1986; Neumeister et al., 2008). However, the noted voltage independency of drug effects in the present study together with the lack of clear drug effect on PPI suggest that a different effector mechanism is regulated by 5-HT$_{5A}$ in the M-cell, probably a cAMP-regulated Cl$^-$ conductance (see above) (Wolszon and Faber, 1989; Noda et al., 2004).

We also considered the possibility that the 5-HT$_{5A}$ antagonists we applied may act nonselectively in the goldfish brain or may act on presynaptic circuits that modulate the M-cell. However, several lines of evidence suggest otherwise. First, two distinct selective antagonists independently produced near-identical effects on the synaptic response and membrane properties of the M-cell. Second, based on its binding affinity, the most likely course of a nonselective effect for SB-6995551 is to act on the 5-HT transporter (5-HTT) (Corbett et al., 2005). However, Mintz and Korn (1991) showed that antagonizing the M-cell 5-HTT produces different postsynaptic effects than were observed with the selective 5-HT$_{5A}$ antagonists used here; thus, these antagonists likely did not act on the 5-HTT. Third, although other 5-HT receptors are expressed in the fish brain, the only 5-HT receptors expressed in the M-cell are 5-HT$_{5A}$ and 5-HT$_6$ (Whitaker et al., 2011). Consistent with a putative postsynaptic action of the 5-HT$_{5A}$ receptor, we observed changes in M-cell resistance after treatment with either 5-HT$_{5A}$ antagonist (Figs. 4, 5). Finally, dosage-driven nonselective effects were an important concern in our experimental design. For that reason, we chose dosages for the drugs that were among the lowest previously reported in the literature with intact animals (Gannon et al., 2009; Kassai et al., 2012). Altogether, we believe the most parsimonious interpretation of the available evidence is that the 5-HT$_{5A}$ receptor plays a modulatory role in the M-cell.

Effects of SB-699551 on startle and PPI

Because PPI is traditionally quantified in behavior, our results could be interpreted as a drug-induced enhancement of PPI attributable to, for example, an increased activity in prepulse inhibitory circuit(s). However, our electrophysiological analysis of PPI at the level of the M-cell (Figs. 3, 4) revealed that the relative magnitude of PPI was unchanged by the application of the 5-HT$_{5A}$ antagonist. Instead, our findings suggest that the antagonist induced a tonic inhibition in the startle circuit that was superimposed on the inhibition evoked by prepulses. In other words, although each of these separate events individually reduced M-cell input resistance, it is their concerted action that effectively pushes the M-cell out of threshold range and consequently reduces startle rate close to zero, manifested as an apparent enhancement of PPI. These separate effects are not easily distinguished at the behavioral level, although the convergence in the magnitude of PPI at different ISIs after drug application (Fig. 1B), (i.e., the elimination of ISI dependencies) can be seen as an indicator

of a drug-induced generalized reduction in excitability. This interpretation was further substantiated in follow-up experiments that directly showed an attenuation in startle rate in non-PPI trials (Fig. 1C).

Importantly, these findings demonstrate that intrinsic properties of the startle circuit can influence the emergence of PPI at the behavioral level. The intrinsic excitability of the startle circuit and the extrinsic mechanisms that produce PPI are commonly interpreted as independent, but our findings are not the first evidence suggesting otherwise. Schicatano et al. (2000) reported that changes in reflex excitability associated with Parkinson's disease effectively modulated PPI of the eyeblink reflex; similarly, in a rodent model, Blumenthal (1997) found that habituation of the startle reflex modulated PPI.

Conversely, extrinsic regulation of startle excitability during PPI by midbrain (and forebrain) circuits is well characterized anatomically (Koch and Schnitzler, 1997; Koch, 1999; Fendt et al., 2001; Yeomans et al., 2006) and physiologically (Bosch and Schmid, 2006, 2008; Yeomans et al., 2010). A consistent finding that has emerged from studies in *ex vivo* rodent preparations is that different neurotransmitters and receptor systems can be linked to discrete components of the PPI time course (Bosch and Schmid, 2006, 2008; Yeomans et al., 2010). Similarly, *in vivo* studies in the M-cell system characterized a time-specific disruption of auditory PPI caused by activation of dopamine receptors (Medan and Preuss, 2011). The present study shows a phasic postsynaptic inhibition that is likely activated by descending (extrinsic) PPI circuits. This phasic inhibition adds to the intrinsic inhibitory tone of the startle circuit. Importantly, it shows that such linear interactions at the synaptic level (Fig. 4C) can produce apparently supralinear behavioral changes (Fig. 1A, black vs gray lines), particularly in an all-or-none startle system such as the M-cell in which a single AP initiates the behavioral response. We believe that these results provide a new perspective to resolve an apparent controversy in the field regarding the significance of intrinsic and extrinsic inhibitory mechanism underlying PPI (Blumenthal, 1997; Schicatano et al., 2000; Sandner and Canal, 2007).

Moreover, together these findings broadly fit the notion that dopaminergic modulation regulates the time course and magnitude of PPI (Medan and Preuss, 2011), whereas 5-HT regulates tonic excitability. This conception may be relevant to the generalized serotonin–dopamine hypothesis that has been advanced to conceptualize neurotransmitter interactions contributing to schizophrenia and the associated deficits in PPI common to schizophrenic populations (Parwani et al., 2000; Braff et al., 2001; Braff, 2010). More generally, our findings also yield a notable tool for future studies of PPI. Specifically, the convergence of PPI magnitude at different ISIs may indicate that, as we found, modulation of PPI is attributable to a nonspecific modulation of startle excitability. Our results emphasize the importance of studying the emergence of PPI on multiple levels, and the M-cell system provides an appropriate model system for such studies.

References

Antonsen BL, Edwards DH (2007) Mechanisms of serotonergic facilitation of a command neuron. J Neurophysiol 98:3494–3504. CrossRef Medline

Arias B, Collier DA, Gast ó C, Pintor L, Gutiérrez B, Vallès V, Fañanás L (2001) Genetic variation in the 5-HT5A receptor gene in patients with bipolar disorder and major depression. Neurosci Lett 303:111–114. CrossRef Medline

Barnes NM, Sharp T (1999) A review of central 5-HT receptors and their function. Neuropharmacology 38:1083–1152. CrossRef Medline

Blumenthal TD (1997) Prepulse inhibition decreases as startle reactivity habituates. Psychophysiology 34:446–450. CrossRef Medline

Bosch D, Schmid S (2006) Activation of muscarinic cholinergic receptors inhibits giantneurones in the caudal pontine reticular nucleus. Eur J Neurosci 24:1967–1975. CrossRef Medline

Bosch D, Schmid S (2008) Cholinergic mechanism underlying prepulse inhibition of the startle response in rats. Neuroscience 155:326–335. CrossRef Medline

Braff DL (2010) Prepulse inhibition of the startle reflex: a window on the brain in schizophrenia. Curr Top Behav Neurosci 4:349–371. CrossRef Medline

Braff DL, Geyer MA, Swerdlow NR (2001) Human studies of prepulse inhibition of startle: normal subjects, patient groups, and pharmacological studies. Psychopharmacology 156:234–258. CrossRef Medline

Burgess HA, Granato M (2007) Sensorimotor gating in larval zebrafish. J Neurosci 27:4984–4994. CrossRef Medline

Corbett DF, Heightman TD, Moss SF, Bromidge SM, Coggon SA, Longley MJ, Roa AM, Williams JA, Thomas DR (2005) Discovery of a potent and selective 5-HT5A receptor antagonist by high-throughput chemistry. Bioorg Med Chem Lett 15:4014–4018. CrossRef Medline

Cordova MS, Braun CB (2007) The use of anesthesia during evoked potential audiometry in goldfish. Brain Res 1153:78–83. CrossRef Medline

Diamond J, Huxley AF (1968) The activation and distribution of GABA and L-glutamate receptors on goldfish Mauthner neurons: an analysis of dendritic remote inhibition. J Physiol 194:669–723. Medline

Diamond J, Roper S, Yasargil GM (1973) The membrane effects, and sensitivity to strychnine, of neural inhibition of the Mauthner cell, and its inhibition by glycine and GABA. J Physiol 232:87–111. Medline

Faber DS, Korn H (1986) Instantaneous inward rectification in the mauthner cell: a postsynaptic booster for excitatory inputs. J Neurosci 19:1037–1043. CrossRef Medline

Faber DS, Fetcho JR, Korn H (1989) Neuronal networks underlying the escape response in goldfish. Ann N Y Acad Sci 563:11–33. CrossRef Medline

Fendt M, Li L, Yeomans JS (2001) Brain stem circuits mediating prepulse inhibition of the startle reflex. Psychopharmacology 156:216–224. CrossRef Medline

Filip M, Bader M (2009) Overview on 5-HT receptors and their role in physiology and pathology of the central nervous system. Pharmacol Rep 61:761–777. Medline

Francken BJ, Jurzak M, Vanhauwe JF, Luyten WH, Leysen JE (1998) The human 5-HT$_{5A}$ receptor couples to G$_i$/G$_o$ proteins and inhibits adenylate-cyclase in HEK293 cells. Eur J Pharmacol 361:299–309. Medline

Fukami Y, Furukawa T, Asada Y (1965) Excitability changes of the Mauthner cell during collateral inhibition. J Gen Physiol 48:581–600. CrossRef Medline

Furukawa T, Ishii Y (1967) Neurophysiological studies on hearing in goldfish. J Neurophysiol 30:1377–1403. Medline

Gannon RL, Peglion JL, Millan MJ (2009) Differential influence of selective 5-HT5A vs 5-HT1A, 5-HT1B, or 5-HT2C receptor blockade upon light-induced phase shifts in circadian activity rhythms: interaction studies with citalopram. Eur Neuropsychopharmacol 19:887–897. CrossRef Medline

Goodfellow NM, Bailey CD, Lambe EK (2012) The native serotonin 5-HT$_{5A}$ receptor: electrophysiological characterization in rodent cortex and 5-HT$_{1A}$-mediated compensatory plasticity in the knock-out mouse. J Neurosci 32:5804–5809. CrossRef Medline

Gotow T, Triller A, Korn H (1990) Differential distribution of serotonergic inputs on the goldfish Mauthner cell. J Comp Neurol 292:255–268. CrossRef Medline

Graham FK (1975) Presidential Address, 1974: the more or less startling effects of weak prestimulation. Psychophysiology 12:238–248. Medline

Hatta K, Korn H (1999) Tonic inhibition alternatives in paired neurons that set direction of fish escape reaction. Proc Natl Acad Sci U S A 96:12090–12095. CrossRef Medline

Hoffman HS, Ison JR (1980) Reflex modification in the domain of startle. I. Some empirical findings and their implications for how the nervous system processes sensory input. Psychol Rev 87:175–189. CrossRef Medline

Hurley PT, McMahon RA, Fanning P, O'Boyle KM, Rogers M, Martin F (1998) Functional coupling of a recombinant human 5-HT5a receptor to G- proteins in HEK-293 cells. Br J Pharmacol 124:1238–1244. CrossRef Medline

Iwata N, Ozaki N, Inada T, Goldman D (2001) Association of a 5-HT(5A) receptor polymorphism, Pro15Ser, to schizophrenia. Mol Psychiatry 6:217–219. CrossRef Medline

Kassaï F, Schlumberger C, Kedves R, Pietraszek M, Jatzke C, Lendvai B, Gyertyán I, Danysz W (2012) Effect of 5-HT5A antagonists in animal models of schizophrenia, anxiety, and depression. Behav Pharmacol 23:397–406. CrossRef Medline

Koch M (1999) The neurobiology of startle. Prog Neurobiol 59:107–128. CrossRef Medline

Koch M, Fendt M (2003) Startle response modulation as a behavioral tool in neuropharmacology. Curr Neuropharmacol 1:175–185. CrossRef

Koch M, Schnitzler HU (1997) The acoustic startle response in rats - circuits mediating evocation, inhibition and potentiation. Behav Brain Res 89:35–49. CrossRef Medline

Korn H, Faber DS (2005) The Mauthner cell a half a century later: a neurobiological model for decision-making? Neuron 47:13–28. CrossRef Medline

Korn H, Burnod Y, Faber DS (1987) Spontaneous quantal currents in a central neuron match predictions from binomial analysis of evoked responses. Proc Natl Acad Sci U S A 84:5981–5985. CrossRef Medline

Medan V, Preuss T (2011) Dopaminergic-induced changes in Mauthner cell excitability disrupt prepulse inhibition in the startle circuit of goldfish. J Neurophysiol 106:3195–3204. CrossRef Medline

Mintz I, Korn H (1991) Serotonergic facilitation of quantal release at central inhibitory synapses. J Neurosci 11:3359–3370. Medline

Nelson DL (2004) 5-HT5 receptors. Curr Drug Targets CNS Neurol Disord 3:53–58. CrossRef Medline

Neumeister H, Szabo TM, Preuss T (2008) Behavioral and physiological characterization of sensorimotor gating in the goldfish startle response. J Neurophysiol 99:1493–1502. CrossRef Medline

Neumeister H, Whitaker KW, Hofmann HA, Preuss T (2010) Social and ecological regulation of a decision-making circuit. J Neurophysiol 104:3180–3188. CrossRef Medline

Noda M, Yasuda S, Okada M, Higashida H, Shimada A, Iwata N, Ozaki N, Nishikawa K, Shirasawa S, Uchida M, Aoki S, Wada K (2003) Recombinant human serotonin 5A receptors stably expressed in C6 glioma cells couple to multiple signal transduction pathways. J Neurochem 84:222–232. CrossRef Medline

Noda M, Higashida H, Aoki S, Wada K (2004) Multiple signal transduction pathways mediated by 5-HT receptors. Mol Neurobiol 29:31–39. CrossRef Medline

Palmer LM, Mensinger AF (2004) The effect of the anesthetic tricaine (MS-222) on nerve activity in the anterior lateral line of the oyster toadfish, *Opsanus tau.* J Neurophysiol 92:1034–1041. CrossRef Medline

Parwani A, Duncan EJ, Bartlett E, Madonick SH, Efferen TR, Rajan R, Sanfilipo M, Chappell PB, Chakravorty S, Gonzenbach S, Ko GN, Rotrosen JP (2000) Impaired prepulse inhibition of acoustic startle in schizophrenia. Biol psychiatry 47:662–669. CrossRef Medline

Pereda AE, Nairn AC, Wolszon LR, Faber DS (1994) Postsynaptic modulation of synaptic efficacy at mixed synapses on the Mauthner cell. J Neurosci 14:3704–3712. Medline

Preuss T, Faber DS (2003) Central cellular mechanisms underlying temperature- dependent changes in the goldfish startle-escape behavior. J Neurosci 23:5617–5626. Medline

Sandner G, Canal NM (2007) Relationship between PPI and baseline startle response. Cogn Neurodyn 1:27–37. CrossRef Medline

Schicatano EJ, Peshori KR, Gopalaswamy R, Sahay E, Evinger C (2000) Reflex excitability regulates prepulse inhibition. J Neurosci 20:4240–4247. Medline

Szabo TM, Weiss SA, Faber DS, Preuss T (2006) Representation of auditory signals in the M-cell: role of electrical synapses. J Neurophysiol 95:2617–2629. Medline

Thomas DR (2006) 5-HT$_{5A}$ receptors as a therapeutic target. Pharmacol Ther 3:707–714. CrossRef Medline

Thomas EA, Matli JR, Hu JL, Carson MJ, Sutcliffe JG (2000) Purtussistoxin treatment prevent 5-HT$_{5A}$ receptor-mediated inhibition of cyclic AMP accumulation in rat C6 glioma cells. J Neurosci Res 61:75–81. CrossRef Medline

Weiss SA, Zottoli SJ, Do SC, Faber DS, Preuss T (2006) Correlation of C-start behaviors with neural activity recorded from the hindbrain in free-swimming goldfish (*Carassius auratus*). J Exp Biol 209:4788–4801. CrossRef Medline

Weiss SA, Preuss T, Faber DS (2009) Phase encoding in the Mauthner sys-

tem: implications in left-right sound source discrimination. J Neurosci 29:3431–3441. CrossRef Medline

Whitaker KW, Neumeister H, Huffman LS, Kidd CE, Preuss T, Hofmann HA (2011) Serotonergic modulation of startle-escape plasticity in an African cichlid fish: a single-cell molecular and physiological analysis of a vital neural circuit. J Neurophysiol 106:127–137. CrossRef Medline

Wolszon LR, Faber DS (1989) The effects of postsynaptic levels of cyclic AMP on excitatory and inhibitory responses of an identified central neuron. J Neurosci 9:784–797. Medline

Yeomans JS, Lee J, Yeomans MH, Steidl S, Li L (2006) Midbrain pathways for prepulse inhibition and startle activation in rat. Neuroscience 142: 921–929. CrossRef Medline

Yeomans JS, Bosch D, Alves N, Daros A, Ure RJ, Schmid S (2010) GABA receptors and prepulse inhibition of acoustic startle in mice and rats. Eur J Neurosci 31: 2053–2061. CrossRef Medline

Zottoli SJ (1977) Correlation of the startle reflex in Mauthner cell auditory responses in unrestrained goldfish. J Exp Biol 66:243–254. Medline